Meteorol. Atmos. Phys. 80, 207–216 (2002)

Meteorology and Atmospheric Physics

[1] Department of Meteorology, Florida State University, Tallahassee, USA
[2] Indian Institute of Tropical Meteorology, Dr. Homi Bhabha Road, Pashan, Pune, India

Impact of nonlocal boundary-layer diffusion scheme on forecasts over Indian region

J. Sanjay[1], P. Mukhopadhyay[2], and S. S. Singh[2]

With 5 Figures

Received November 16, 2001
Revised December 28, 2001

Summary

The results of incorporating a nonlocal boundary-layer diffusion scheme in a forecast model over Indian region are discussed. The simple formulation of atmospheric boundary layer height in the nonlocal diffusion scheme is examined in detail to understand how far the model simulated boundary layer height is realistic. Analyses of the temporal and spatial variability of the boundary height for three cases representing premonsoon, active monsoon and post monsoon conditions over Indian region show that it is comparable with the observational evidence. Further, for a case of active monsoon condition over Indian region, comparison of precipitation forecasts with the nonlocal scheme and the control local boundary-layer scheme clearly indicated that the model run with the nonlocal scheme is significantly more accurate in forecasting the intense precipitation locations.

1. Introduction

Turbulent motions within the atmospheric boundary layer (BL) are primarily responsible for the mixing of heat, moisture and momentum. Large scale numerical models conventionally describe this turbulent mixing with a vertical diffusion scheme using an eddy diffusivity determined independently at each point in the vertical based on local vertical gradients of wind and virtual potential temperature. This approach assumes that turbulent fluxes always flow down the mean gradient. The fact that such turbulence closures fail in the case of well-mixed convective boundary layers was recognized long time ago. Based on experimental evidence, Deardorff (1972) gave theoretical explanation to the failure of this down gradient approximation for convective turbulence. The presence of large coherent structures such as convective thermals can produce turbulent transports that cause fluxes to go counter to the local gradient. A simple formulation including the countergradient effects for vertical diffusion was developed by Troen and Mahrt (1986). This scheme has been widely tested in numerical models with suitable modifications (Holtslag and Boville, 1993; Hong and Pan, 1996, and others). This nonlocal vertical diffusion scheme determines an eddy-diffusivity profile based on a diagnosed boundary-layer height and a turbulent velocity scale. It also incorporates nonlocal (vertical) transport effects for heat and moisture. Testing in climate models (e.g., Holtslag and Boville, 1993) showed that the temperature and moisture profiles were better simulated by this scheme than the local diffusion scheme. It increased the vertical moisture transport causing more rapid detrainment from the boundary-layer top and, as a consequence, shifting of the maximum cloudiness to upper regions above the boundary layer. Also it was seen that

this scheme induced an overall increase in total precipitation amounts. Hong and Pan (1996) showed that introduction of a nonlocal boundary vertical diffusion scheme and update of the convection scheme in the National Centers for Environmental Prediction (NCEP) Medium Range Forecast (MRF) model improved precipitation forecast skill over continental USA.

In this paper, we present the results of testing the nonlocal scheme following Hong and Pan (1996) in a version of the Global Spectral Model (GSM) run operationally at National Center for Medium Range Weather Forecasts (NCMRWF), India. We focus on the simulation of the characteristics of BL development with the nonlocal scheme over the Indian region for three cases during pre-monsoon, active summer monsoon and post monsoon and attempt to validate with observational evidence. In addition, for the case of active monsoon condition over Indian region, the three day forecasts with the nonlocal scheme are compared to the control local boundary layer scheme run to see the impact on the forecasted low level wind circulation and rainfall.

Section 2 gives a brief description of the model and the boundary layer schemes used. Data utilized and the experiments carried out are described in Sect. 3. Section 4 contains a detailed examination of the temporal and spatial variability of the simulated BL height. This section also discusses on the results of a synoptic forecast obtained with the local and nonlocal schemes and makes a quantitative assessment of the precipitation forecasts. Conclusions are presented in Sect. 5.

2. Description of the model

In this section, we present the salient features of the GSM used and a brief description of the modifications made to the boundary-layer scheme following Hong and Pan (1996).

The model used is a version of the operational forecast model at NCMRWF. This is an adapted version of the earlier NCEP GSM (documented in NMC Staff, 1988). It is based on the primitive equations. The model variables are vorticity, divergence, virtual potential temperature, natural logarithm of surface pressure and specific humidity. The prediction equations consist of the divergence and vorticity equations, the hydrostatic equation, the thermodynamic equation, the mass continuity equation and conservation equation for water vapor. The model uses spherical harmonic functions for the horizontal representation of variables. The vertical co-ordinate system is the sigma co-ordinate, with a finite difference scheme of Arakawa. The scheme conserves mass, momentum, potential temperature, water vapor, angular momentum and total energy. The time integration scheme is semi implicit to allow longer time steps. The model horizontal resolution is T80, corresponding to a grid size of about 1.5 degrees or 160 km. The model has 18 vertical levels, the lowest being about 10 hPa above the surface and with five levels below 850 hPa.

The physical processes used in the model include long- and short-wave radiation, cloud-radiation interaction, planetary boundary-layer processes, deep and shallow convection, large scale condensation, gravity wave drag, enhanced topography, simple hydrology, and vertical and horizontal diffusions. The deep convection scheme follows a modification of the Kuo scheme. The surface layer physics is based on the Monin-Obukhov similarity theory (NMC Staff, 1988). Soil wetness is predicted based on the bucket method. Snow depth is predicted and interacts with radiation through surface albedo. Surface evaporation is based on Penman-Monteith theory. Over land, surface temperature and soil temperature (two layers) are predicted using energy balance.

A local stability-dependent vertical diffusion scheme was originally used in the model for the boundary layer as well as the free atmosphere. In this scheme the vertical turbulent transport of momentum, heat, and moisture is represented by an eddy diffusion term of the form:

$$F_c = -K_c \partial C/\partial z, \tag{1}$$

where, $\mathbf{F_c}$ is the vertical flux for the quantity C (e.g., wind components $\mathbf{u}$ and $\mathbf{v}$, potential temperature $\boldsymbol{\theta}$, and water vapor mixing ratio $\mathbf{q}$), $\mathbf{z}$ is the vertical co-ordinate, and $\mathbf{K_c}$ is the vertical eddy diffusion coefficient, or eddy diffusivity. The eddy diffusivity used in this formulation depends on the local vertical wind shear, the parcel mixing length, and the local Richardson number. Betts et al. (1996) gives a detailed description of this local diffusion scheme.

In this study a nonlocal boundary layer scheme following Hong and Pan (1996) is incorporated

and tested in the model. The representation of the vertical eddy flux within the boundary layer in this scheme is given by

$$F_c = -K_c(\partial C/\partial z - \gamma_c), \tag{2}$$

where $\boldsymbol{\gamma_c}$ is a "countergradient" transport term describing nonlocal transport for $\boldsymbol{\theta}$ and $\mathbf{q}$. The eddy diffusivity for momentum by the nonlocal formulation is given as

$$K_m = kw_m z\left(1 - \frac{z}{h}\right)^2, \tag{3}$$

where $\mathbf{w_m}$ is a mixed-layer velocity scale that depends on the surface friction velocity, the surface layer height (0.1 h), and the Monin-Obukhov length, and $\mathbf{h}$ is the boundary-layer height.

The eddy diffusivities for temperature and moisture ($\mathbf{K_t}$) are computed using the Prandtl number relation. More details on the formulations of the various terms present in these equations and other aspects of the scheme can be found in Hong and Pan (1996). The nonlocal diffusion approach is used in the model up to the boundary layer top. Above this layer, the local diffusion approach is applied with modified stability functions (see Hong and Pan, 1996).

3. Data and experiments

Initial conditions to the model obtained from the operational global data assimilation and analysis system at NCMRWF is used for experiments in this study. The verifying raingauge station data used is the accumulated precipitation amounts for each 24-hour period ending at 0300 UTC provided by India Meteorological Department (IMD). Three cases representing pre-monsoon, active summer monsoon and post monsoon conditions over Indian region are chosen. Three day forecast experiments with the local scheme (LD) and the nonlocal scheme (NLD) using 0000 UTC of 04 April 1996 (pre-monsoon), 25 July 1996 (summer monsoon) and 6 November 1995 (post-monsoon) initial conditions were carried out.

4. Discussion of results

4.1 Boundary-layer height

The key quantity in the nonlocal BL scheme is the BL height ($\mathbf{h}$), which is computed explicitly as

$$h = \frac{Rib_{cr}\theta_{va}|V_h|^2}{[g(\theta_{vh} - \theta_s)]}, \tag{4}$$

where $\mathbf{Rib_{cr}}$ is a critical bulk Richardson number, $\mathbf{V_h}$ and $\boldsymbol{\theta_{vh}}$ are the horizontal wind speed and the virtual potential temperature at the top of the boundary layer, $\mathbf{g}$ is the gravity, $\boldsymbol{\theta_{va}}$ is the virtual potential temperature at the lowest model level and $\boldsymbol{\theta_s}$ is the temperature of the air near the surface which is modified to include the influence of thermals for the unstable case.

Figure 1 shows the diurnal variation of BL height at selected stations (nearest grid points) over Indian region in three-day forecasts for the three cases chosen. Figure 1a–d is for four continental grids near New Delhi, Anand, Kharagpur and Bangalore representing differing geographical locations across the country. Also shown are two oceanic grids (Fig. 1e, f) over the adjoining central Arabian Sea and Bay of Bengal to visualize $\mathbf{h}$ variation over ocean. The BL response to diurnal heating over land is evident, especially during the pre-monsoon dry convective case shown by solid lines in the figure. The diurnal range is found to be a minimum during the active monsoon case shown by dashed lines. During the post monsoon case shown by dotted lines, the diurnal range are found to be higher than that for the monsoon case over the continental grids. In all the cases, the BL height generally remains near its minimum throughout the night, increases during daytime and reaches to a maximum at the time of maximum insolation, and then rapidly decreases at sunset. The simulated diurnal variation is found largest for the grid point near Delhi (Fig. 1a) during the pre-monsoon case. The maximum height attained is over 5 km, which is slightly higher than the estimated value of over 4 km for Delhi station and its surroundings by Gamo et al. (1994). Raman et al. (1990) observed that the BL height over Delhi could reach 4.7 km during dry conditions. The other land stations show maximum BL height in the range of 3 to 4 km only which indicates that the strongest dry convection occurs over North India. Over the selected oceanic grids (Fig. 1e, f) the BL heights are found to be less than 0.5 km during the pre-monsoon case with no significant diurnal variation, which can be attributed to the use of fixed sea surface temperatures in these experiments.

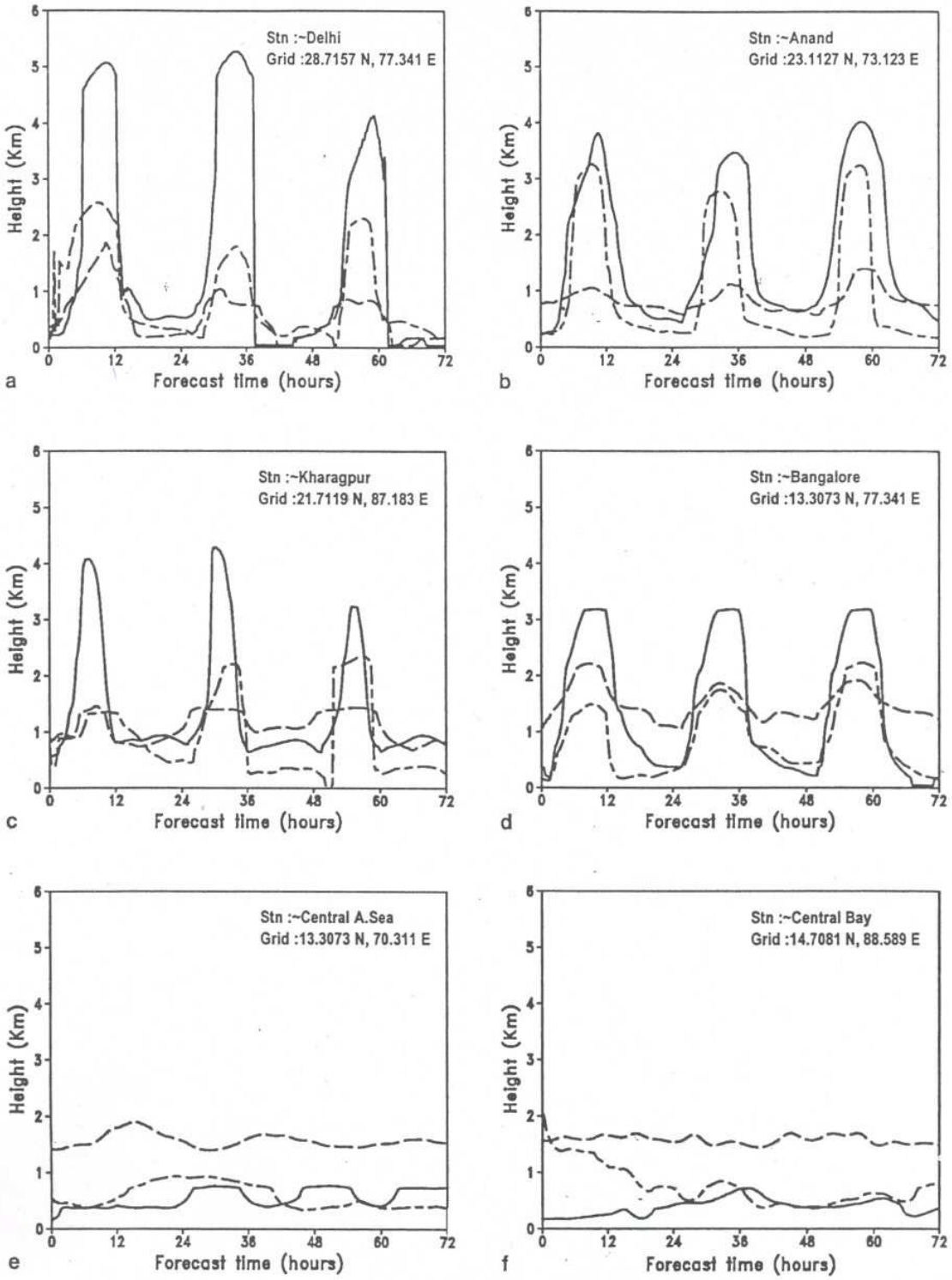

Fig. 1. Diurnal variation of boundary layer height(km) at various model grid points for different model inputs: 0000 UTC of 05 April 1996 (solid line); 25 July 1996 (dashed line); 25 November 1995 (dash-short dash line)

During the active monsoon case the BL height maxima is found to be relatively low over all continental grids with values ranging from 1 to 2 km. These are in the general range shown by various observational studies during Monsoon Trough Boundary-Layer Experiment (MONTBLEX) in 1990 (Narasimha et al., 1990). The height of monsoon BL at Bangalore was observed to be about 0.9 km during daytime convective conditions by Raman et al. (1990). The oceanic grids show BL heights of about 1.5 km during the active monsoon case, which are much higher than that obtained for the pre-monsoon case. Holt and Raman (1987) observed that the mean virtual potential temperature profiles in the BL over central Arabian Sea and north central Bay of

Bengal during onset and active monsoon periods were more unstable than those during break or pre-monsoon conditions indicating a higher mixed layer during active monsoon. They attributed this to a marked increase in surface heat fluxes during the active monsoon period. Our results also show enhanced surface heat fluxes (figure not shown) for the oceanic grids during the active monsoon case supporting the higher BL heights obtained for this case.

To understand the simulated spatial variation, the three-day mean and diurnal ranges of the BL height for the three cases are shown in Fig. 2. The diurnal range was determined from the

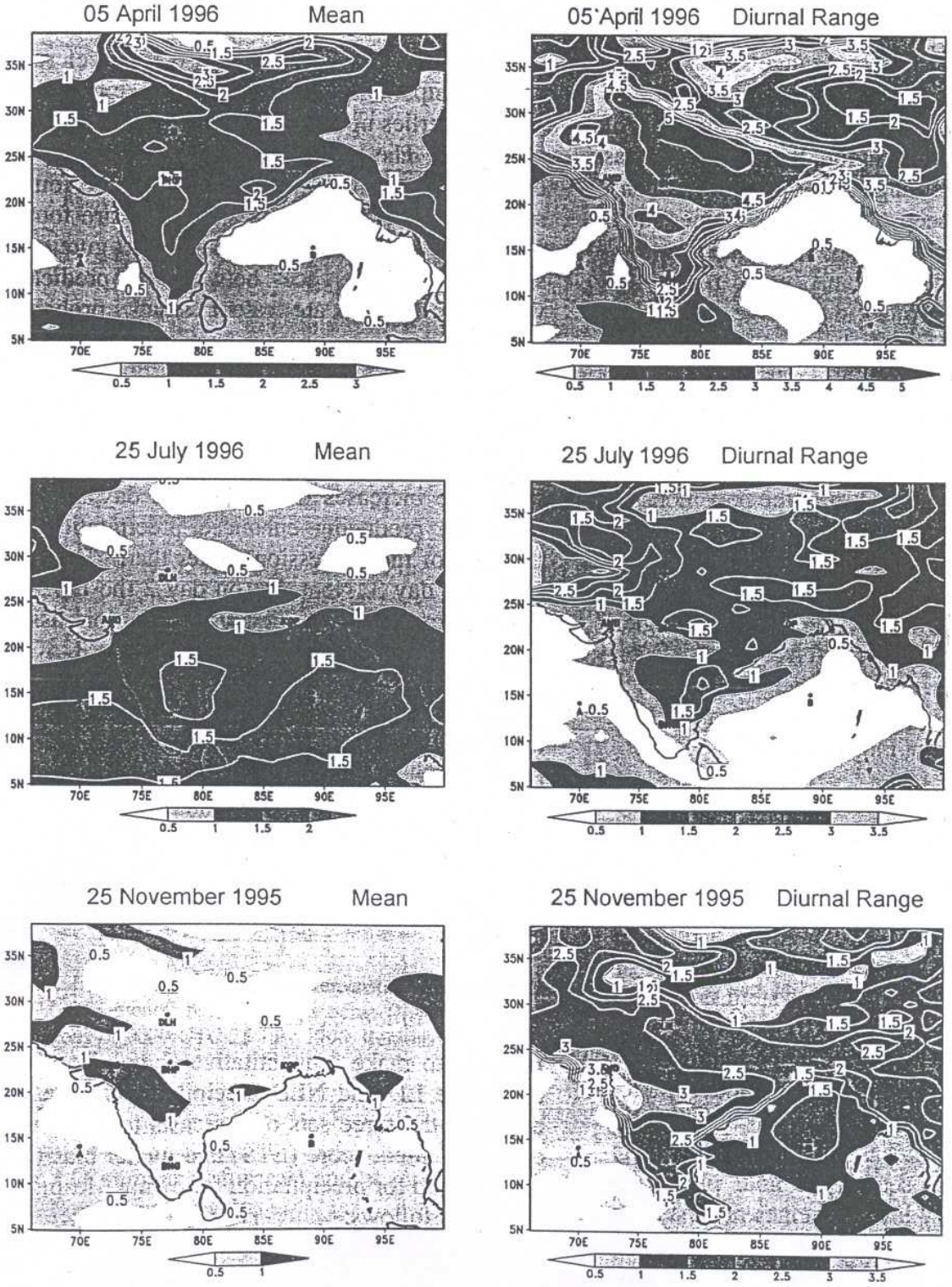

Fig. 2. Three day mean and diurnal range of simulated boundary layer height(km). Contour interval 0.5 km, shading above 0.5 km

maximum and minimum values of BL height based on each model time step (15 minutes) data for the entire forecast period. Similar to the distribution of BL height over the individual grid points, the mean BL height and diurnal range are found to be a maxima for the premonsoon case. While the mean heights are found to be in the range of 1 to 2 km (shaded regions in the figure are greater than 0.5 km), the diurnal ranges exceeds 3 km over most of the Indian land mass. Over North India the diurnal range shows a maximum exceeding 5 km, which seems realistic as the solar heating is maximum during this time of the year. Over oceanic region, the mean values as well as the diurnal ranges are very low. A complete contrast is seen during the summer monsoon period with the maximum mean values shifting southward over the oceanic region and the diurnal ranges reducing drastically to less than 2 km over most of the continental region. This reduction in BL heights over India was also noted by Kusuma et al. (1991), which they noted may be due to the presence of high water vapor content and cloudy conditions prevalent during active monsoon period. During the post monsoon period the mean values are about 1 km, while the diurnal range picks up to more than 2 km over most of the land points with range exceeding 4 km located over the northwestern dry region. Thus, in general, it can be inferred that the simulated diurnal variation of BL height by the nonlocal BL scheme is fairly in agreement with the observed values over Indian region.

4.2 Synoptic forecasts

During 25 to 28 July 1996 active monsoon condition existed over Indian region with the northwestward movement of a monsoon depression after its formation over northwest Bay of Bengal. Associated with this synoptic system heavy precipitation of about 5 to 10 cm day^{-1} were reported by some IMD raingauge stations over central India. To compare the model performance with the local and nonlocal boundary layer schemes in forecasting this heavy precipitation event, three sets of 72 hour predictions with both boundary layer schemes are made beginning at three consecutive 12 hour apart initial conditions namely 0000 and 1200 UTC of 25 and 0000 UTC of 26 July 1996. The low-level cyclonic circulation features, the movement of the system and the predicted precipitation patterns in the first set of forecast are examined in detail.

Figure 3 depicts the predicted Day 1, Day 2 and Day 3 low level (850 hPa) wind circulation (vectors) and the 24 hour accumulated total precipitation amounts (contours) over Indian region for the local scheme (LD) and nonlocal scheme (NLD) model runs with the initial conditions of 0000 UTC 25 July 1996. Both model runs show comparable features of wind circulation with westerlies up to 20° N and weaker easterlies northward. The location of the cyclonic circulation and its northwestward movement are found similar in both the forecasts and also are found closer to the verification analyses (figure not shown). The differences between the predicted wind circulations are rather small, probably because both the boundary-layer schemes use a down gradient formula for wind diffusion without any nonlocal terms.

Precipitation forecasts (Fig. 3) show differences between LD and NLD model runs. The difference increases from day 1 to day 3, with NLD run producing enhanced precipitation to the west of the depression center than LD model run by day 3. Note that on day 2 the LD run did not capture the heavy precipitation associated with the cyclonic system. On day 3, a region of spurious heavy precipitation seen to the east of the cyclonic center in the LD run is found to be completely removed in the NLD run suggesting that the nonlocal approach substantially improves the precipitation forecast by enhancing the convective overturning at the right location and by suppressing spurious precipitation as is also noted by Hong and Pan (1996).

4.3 Precipitation scores

In order to make a quantitative comparison between the LD and NLD precipitation forecasts, using all the three sets of forecasts together the equitable threat score (ETS) and model bias (B) is computed for precipitation following Mesinger (1996) as follows:

$$ETS = \frac{H - E}{F + O - H - E} \quad and \quad B = \frac{F}{O}$$

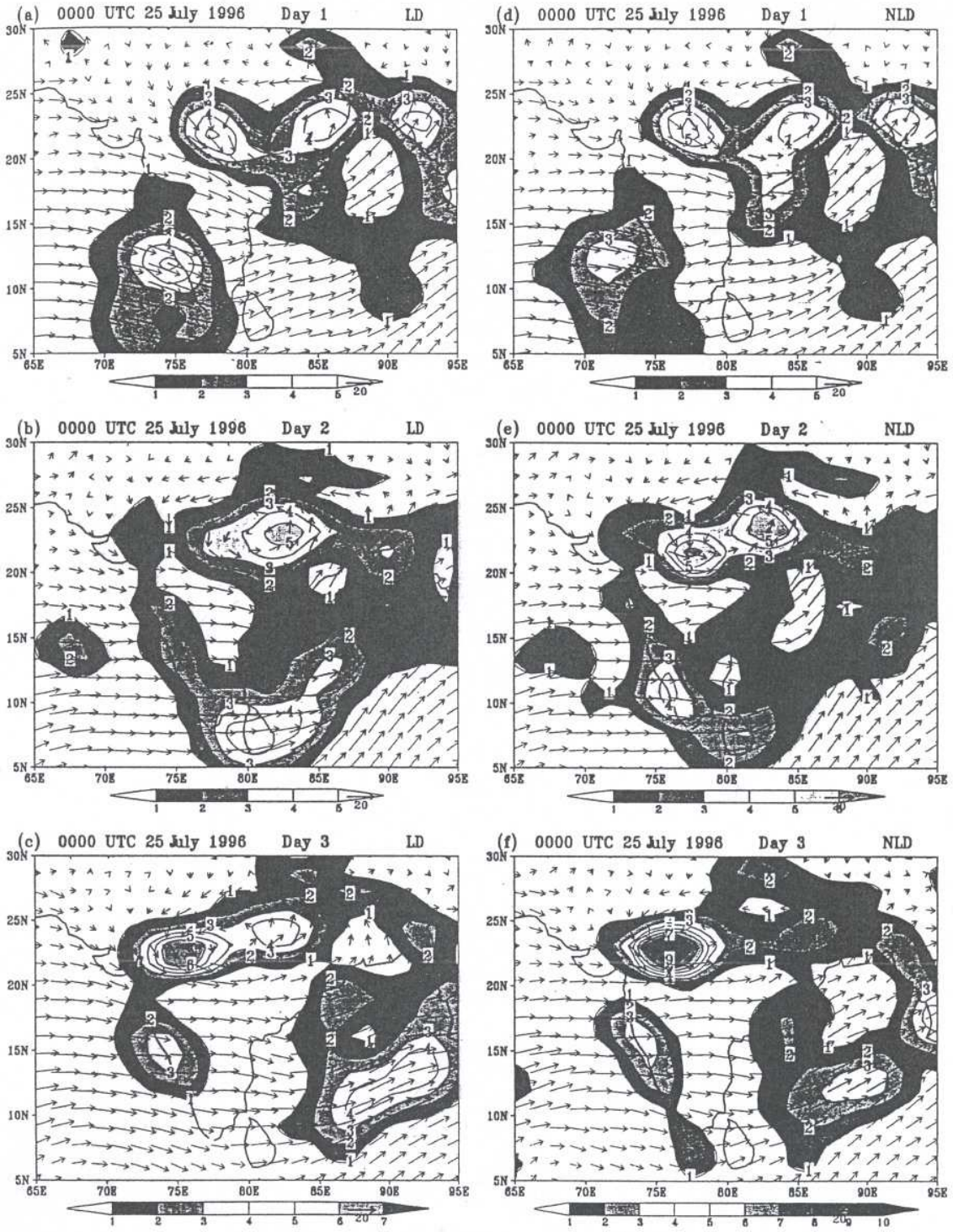

Fig. 3. Day 1, Day 2 and Day 3 forecasts of 850 hPa wind (m s^{-1}) [vectors] and 24 hour accumulated precipitation (cm day^{-1}) [contours] for the local scheme (LD) [left panel] and the nonlocal scheme (NLD) [right panel] with the initial conditions of 0000 UTC 25 July 1996. Regions of precipitation more than 2 cm day^{-1} are shaded

here,

H number of correctly forecast points (hits),
F and **O** number of forecast and observed model grid boxes respectively,
$E = \frac{F \cdot O}{N}$, the expected number of hits in a random forecast, and,
N total number of points being verified.

Mesinger (1996) discusses that ETS can be said to represent the fractional number of correctly forecasted points of a precipitation event above random, normalized by the total number of observed and/or forecast points, also above the number of hits in a random forecast. ETS has a range between 0 and 1. The observed raingauge

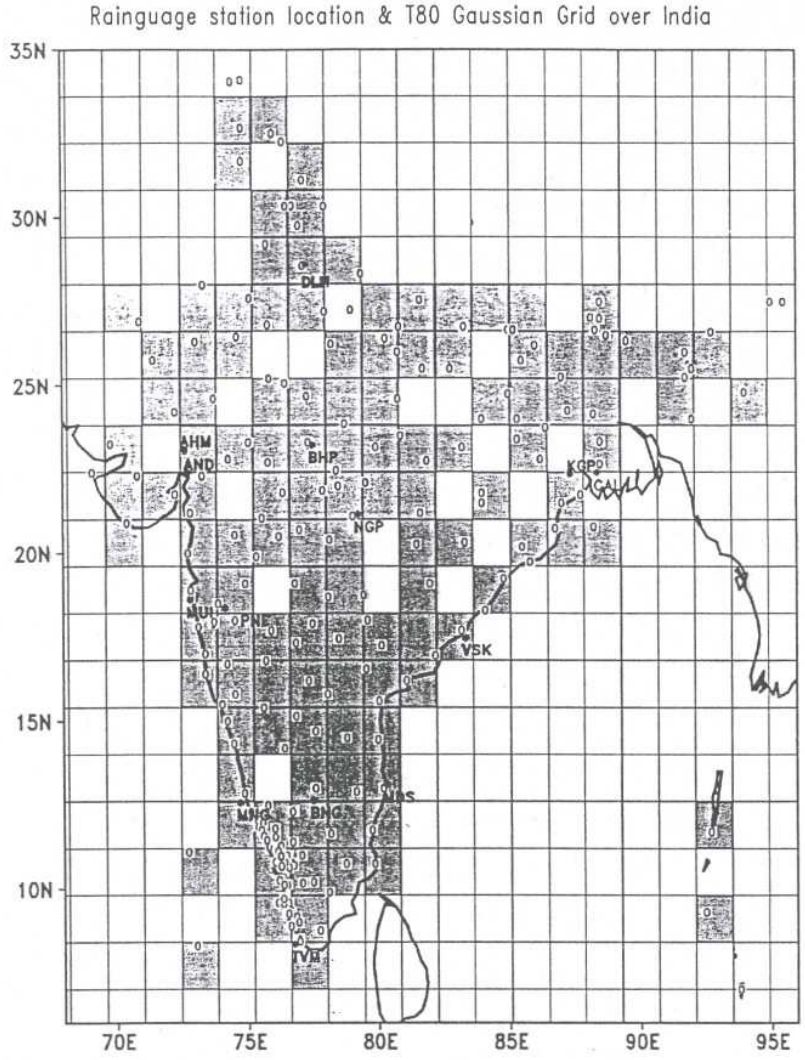

Fig. 4. Location of the raingauge stations (circles) and the selected T80 spectral model grid boxes (shaded) for precipitation skill score computation over Indian region

station reports are simple box averaged within the model gaussian (T80) grid boxes. Only grid boxes with at least one station report is used for computation of scores. Figure 4 shows the location of the raingauge stations (circle) and the selected model grid boxes (shaded) over India, which comprises of 124 verification boxes. The forecast total precipitation amounts for each 24-hour period ending 0300 UTC from the series of 72-hour predictions are used for computing precipitation scores. With three forecasts, we have a total of 6 verifications over the two 24 hour verification periods ending 0300 UTC of 27 and 28 July 1996. In the upper panel of Fig. 5 we show the total ETS for the NLD (solid line) and LD (dashed line) model runs for the entire period. The threshold amounts of precipitation for which the scores are plotted are 0.25, and 1.0 to 9.0 cm in 24 hour. Each threshold actually represents the given amount and all amounts greater. It is clear that for heavier precipitation (5 cm day^{-1} and above) categories, NLD produces higher ETS than the LD model run, suggesting that the forecasts using nonlocal scheme were significantly more accurate in predicting quantities and locations of precipitation than the local scheme forecasts. It may also be noted that for the LD run there is no skill beyond a threshold of 7 cm day^{-1}. The model bias score (B) shown in the lower panel of Figure 5 indicates that for both runs the model has a moist bias ($B > 1$) up to 4 cm day^{-1} thresholds and a drier bias ($B < 1$) for heavier precipitation thresholds. But it is seen that at all levels of intensity, except less than 1 cm day^{-1}, the NLD run show lesser bias suggesting that the nonlocal scheme did not produce higher ETS simply by covering larger areas of precipitation than the local scheme forecasts.

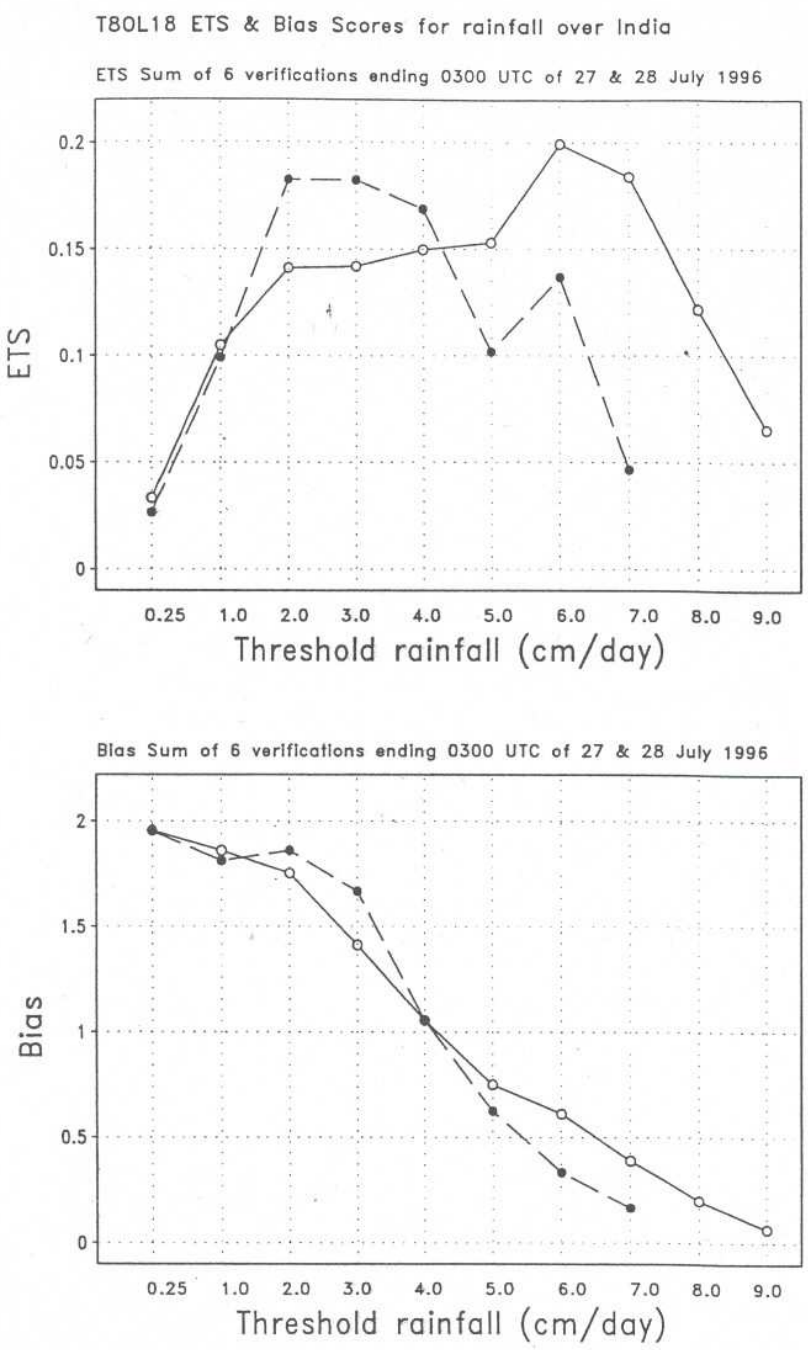

Fig. 5. Equitable threat scores (ETS) for a total of three consecutive forecasts run with the nonlocal scheme (solid lines) and the local scheme (dashed lines), upper panel. Bias scores for the same set of forecasts, lower panel

5. Concluding remarks

This study examined the performance of a nonlocal boundary-layer diffusion scheme for three cases representing premonsoon, active monsoon and post-monsoon conditions over Indian region. It was shown that the diagnostic formulation for boundary-layer height used in the nonlocal scheme is able to bring out realistic features of temporal and spatial variability of atmospheric boundary layer over Indian region.

For a case of active monsoon condition over Indian region the impact on forecast accuracy of the nonlocal boundary-layer diffusion scheme in the global forecast model versus the commonly used local diffusion approach was examined. This was done by a synoptic examination of the differences in a set of forecasts, and by comparison of precipitation skill scores in three sets of consecutive forecasts performed using the local and the new nonlocal boundary-layer schemes. Both efforts indicated that greater accuracy in precipitation forecasts is achieved with the nonlocal scheme.

It would have been desirable to consider more cases of heavy precipitation events for this comparison. In this case study the precipitation is

associated with a monsoon depression which involves a wide variety of dynamic and thermodynamic forcing. It is likely that the results would be the same if extended to more similar case studies. We hope to report on this issue in the near future by testing the nonlocal boundary-layer diffusion scheme in a high resolution FSU Global Spectral Model (Krishnamurti et al., 1998) used for real time numerical weather predictions.

Acknowledgements

The model code and initial conditions provided by NCMRWF is acknowledged with thanks. Dr. Song-You Hong, NCEP has kindly provided the code of the NCEP nonlocal boundary layer diffusion scheme. For the present model comparison the Indian station rainfall reports were obtained from IMD. The first author sincerely acknowledges the Director, Indian Institute of Tropical Meteorology, Pune for giving him an opportunity to carryout part of this study at FSU. He also acknowledge the scientific help and encouragement received at various stages of the study from Prof. T. N. Krishnamurti, Arun Chakraborty, T. S. V. Vijaya Kumar, Nihat Cubukcu and Darlene Oosterhof, scientists working in Dr. Krishnamurti's research laboratory. This study was funded by NASA grant number NAG8-1537.

References

Betts AK, Hong S-Y, Pan H-L (1996) Comparison of NCEP-NCAR reanalysis with 1987 FIFE data. Mon Wea Rev 124: 1480–1498

Deardorff JW (1972) Theoretical expression for the countergradient vertical heat flux. J Geophys Res 77: 5900–5904

Gamo M, Goyal P, Manjukumari Mohanty, UC, Singh MP (1994) Mixed-layer characteristics as related to the monsoon climate of New Delhi, India. Boundary-Layer Meteorol 67: 213–227

Holt and Raman (1987) A study of mean boundary-layer structures over the Arabian Sea and Bay of Bengal during active and break monsoon periods. Boundary-Layer Meteorol 38: 73–94

Holtslag AAM, Boville BA (1993) Local versus nonlocal boundary layer diffusion in a global climate model. J Clim 6: 1825–1847

Hong S-Y, Pan H-L (1996) Nonlocal boundary layer vertical diffusion in a medium-range forecast model. Mon Wea Rev 124: 2322–2339

Krishnamurti TN, Bedi HS, Han W (1998) Organization of convection and monsoon forecasting. Meteorol Atmos Phys 65: 171–181

Kusuma GR, Sethu Raman, Prabu A (1991) Boundary-layer heights over the monsoon trough region during active and break phases. Boundary-Layer Meteorol 57: 129–138

Mesinger F (1996) Improvements in quantitative precipitation forecasts with the Eta regional model at the NCEP: The 48-km upgrade. Bull Amer Meteor Soc 77: 2637–2649

Narasimha R, Sikka DR, Prabhu A (1997) The monsoon trough boundary-layer. Bangalore Indian Academy of Sciences, 422 pp

NMC Development Division 1988: Documentation of the research version of the NMC Medium-Range Forecasting Model, 504 pp

Raman S, Templeman B, Templeman S, Holt T, Murthy AB (1990) Structure of the Indian southwesterly pre-monsoon and monsoon boundary layers: Observations and numerical simulations. Atmos Env 24A: 723–734

Troen and Mahrt (1986) A simple model of the atmospheric boundary layer. Sensitivity to surface evaporation. Boundary-Layer Meteorol 37: 129–148

Authors' addresses: Sanjay Jayanarayanan, Department of Meteorology, Florida State University, Tallahassee, FL–32306, USA (E-mail: sanjay@io.met.fsu.edu); P. Mukhopadhyay and S. S. Singh, Indian Institute of Tropical Meteorology, Dr. Homi Bhabha Road, Pashan, Pune, India